Inorganica Chimica Acta 439 (2016) 1–7

Contents lists available at ScienceDirect

Inorganica Chimica Acta

journal homepage: www.elsevier.com/locate/ica

A naphthalene derived Schiff base as a selective fluorescent probe for Fe^{2+}

S. Santhoshkumar [a], K. Velmurugan [a], J. Prabhu [a], G. Radhakrishnan [b], R. Nandhakumar [a,*]

[a] Department of Chemistry, Karunya University, Karunya Nagar, Coimbatore 641 114, Tamil Nadu, India
[b] CSIR – Central Electro Chemical Research Institute, Karaikudi 630 006, India

ARTICLE INFO

Article history:
Received 17 July 2015
Received in revised form 15 September 2015
Accepted 24 September 2015
Available online 9 October 2015

Keywords:
Schiff base
Chemosensor
Fluorescence
ICT
Fe^{2+} detection
Water analysis

ABSTRACT

A naphthalene pyridine Schiff base **1** as a fluorescent chemosensor was developed for the detection of Fe^{2+} ions in CH_3CN–H_2O solution. Its binding properties toward various other heavy and transition metal ions including Fe^{3+} ions were examined. The sensor showed high selectivity and sensitivity towards Fe^{2+} ions in aqueous media with the lower detection limit of 1.5×10^{-7} M. The fluorescence "turn-on" recognition process follows the ICT process and C=N isomerisation. In addition, determination of Fe^{2+} in a variety of samples were analyzed which includes commercially available tablets, tomato juice, dark chocolate and tap water.

1. Introduction

The development of fluorescent chemosensors for specific detection of various transition metal ions is challenging to current researchers due to the potential applications in medicine as well as environmental research domains [1–5]. Among them, iron is one of the most essential metal ions in our living systems. In biological network, it plays a critical role in living organisms such as oxygen metabolism, oxygen uptake and electron transfer process. Furthermore, iron present as a cofactor in various enzymatic reactions and easy redox reactions between Fe^{2+} and Fe^{3+} [6–13]. However, excess or deficiency of Iron leads to serious diseases, such as lipid peroxidation, DNA fragmentation leads to cell death, liver damage, kidney failure, anemia, cancer, Alzheimer's, and Parkinson's diseases [14–17]. Higher level of iron exists in the protein-bound form; labile iron and non-protein bound iron were reported to involve healthy and diseased states in living organisms [18–20]. Therefore, the demand for rapid detection and discrimination of Fe^{2+} from other ions including Fe^{3+} at lower concentration has significant applications in environment and biological systems [21,22].

Presently, many techniques are available for the detection of Fe^{2+} such as colorimetry, atomic absorption spectroscopy, voltammetry, spectrophotometry, and flow injection [23–27]. Above methods is very complicated, tedious sample preparation and required sophisticated instrumentation [28–30]. On the other hand, fluorescent chemosensors overcome all those problems than other methods due to their simplicity, low-cost, sensitivity, and instantaneous response and capable of specific recognition of particular ions [31–35]. Fluorescent probes for iron is a challenging one because of its effective fluorescence quenching nature as well as its different oxidation and spin states. Highly reactive iron exists as ferrous ion (Fe^{2+}) than ferric ion (Fe^{3+}) due to its better water solubility, intracellular reductive environment and good binding affinity [36–40]. Besides, Fe^{2+} is a potential catalyst for chemical reactions, producing harmful labile oxygen species [41–43]. In addition, fluorescent probes for Fe^{2+} with a turn-on response, are highly desirable for understanding both the physiological and pathological roles. Even if, there are many reports are available for turn-on Fe^{2+} and Fe^{3+} probes [44–51] but Fe^{2+}-responsive turn-on with red shift based charge transfer fluorescent probes not available to date. Therefore, the development of selective sensing of Fe^{2+} and implementing a new method to quantify trace level of Fe^{2+}-ions in environmental systems is current focus of our research.

* Corresponding author.
E-mail address: nandhakumar@karunya.edu (R. Nandhakumar).

http://dx.doi.org/10.1016/j.ica.2015.09.030
0020-1693/

According to supramolecular concepts, naphthalene was chosen as a fluorophore and pyridine used as an ionophore due to their excellent photo-physical properties, high fluorescence quantum yield and good coordination ability [52–54]. Herein, we designed and synthesized a new class of naphthalene based fluorescent chemosensor (**1**) which exhibits selective sensing towards Fe^{2+} with remarkable fluorescence turn-on with red shifted response *via* Intramolecular Charge Transfer (ICT) process in $CH_3CN–H_2O$ (1:1 v/v, HEPES = 50 mM, pH = 7.4) solutions.

2. Experimental

2.1. Materials and instruments

All solvents were purchased commercially with reagents grade quality. 2-aminopyridine and 1-naphthaldehyde were obtained from Sigma. ^1H NMR and ^{13}C NMR spectra were recorded on a Bruker 300 and 100 MHz spectrometer using $CDCl_3$ and DMSO-d_6 solutions with TMS as internal standard. LC–MS was determined on a LC-MSD-Trap-XCT Plus based on infusion methods. Absorption spectra were recorded on a Shimadzu UV-240 spectrophotometer. Fluorescence measurements were performed on a Jasco FP-8200 spectrofluorometer equipped with quartz cuvettes of 1 cm path length. The excitation and emission slit widths were 5.0 nm. All absorption and emission spectra were recorded at 24 ± 1 °C. Stock solutions for analysis were prepared (2×10^{-3} M for compound **1** (CH_3CN/H_2O, 1:1 (v/v), HEPES = 50 mM, pH = 7.4) immediately before the experiments. The solutions of metal ions were prepared from chloride and nitrate salts of Pb^{2+}, Cu^{2+}, Cd^{2+}, Hg^{2+}, La^{3+}, Zn^{2+}, Co^{2+}, Ni^{2+}, Ca^{2+}, Mn^{2+}, Cr^{3+}, Ba^{2+}, Ce^{3+}, Mg^{2+}, Al^{3+}, Fe^{2+}, Fe^{3+}, Ag^{+}, Na^{+} and K^{+}. The studies on the binding properties of **1** were carried out in solution (CH_3CN/H_2O, 1:1 (v/v), HEPES = 50 mM, pH = 7.4). The different metal ion solutions (100 equiv.) were prepared by dissolving the desired amount of metal salts in solution (CH_3CN/H_2O, 1:1 (v/v), HEPES = 50 mM, pH = 7.4). The fluorescence titration was performed with a series of 4×10^{-6} M solutions of **1** containing various equivalents of Fe^{2+}-ions. Binding studies were confirmed by job's plot and nonlinear curve fitting methods.

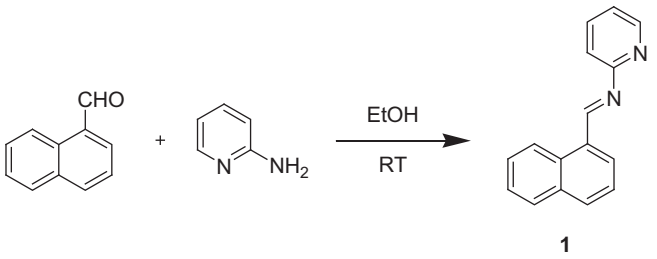

Scheme 1. Synthesis of receptor **1**.

2.2. Synthesis

2.2.1. Synthesis of (E)-N-(naphthalene-1-ylmethylene)pyridine-2-amine (1)

1-Naphthaldehyde (0.5 g, 3.20 mmol) was dissolved in ethanol (20 mL) in the presence of 2-aminopyridine (0.36 g, 3.84 mmol) and stirred for 5 h at room temperature. The reaction mixture was allowed to settle down, and the precipitate formed was filtered and recrystallized from methanol to afford the compound **1** as a white colour solid (90% yield). M.p. 232 °C, ^1H NMR (300 MHz, $CDCl_3$): 9.59 (s, 1H), 8.54–8.56 (d, 1H), 8.20–8.24 (d, 1H), 8.08–8.11 (d, 1H), 8.02–8.05 (d, 1H), 7.37–7.98 (m, 5H), 7.18–7.25 (m, 2H) ppm. ^{13}C NMR (100 MHz, DMSO-d_6): 109.15, 114.81, 115.74, 118.81, 119.46, 120.19, 123.16, 126.84, 127.18, 127.72, 127.94, 128.86, 135.29, 141.55, 155.67, 166.47 ppm. *Anal.* Calc. for $C_{16}H_{12}N_2$: C, 82.73; H, 5.21; N, 12.06. Found: C, 82.15; H, 5.02; N, 12.10%. LC–MS calcd. for $C_{16}H_{12}N_2$: $[M^+]$ 232, found $[M^+{+}H]^+$ 233.

3. Results and discussion

3.1. Synthetic design of chemosensor *1*

The one step synthesis of the naphthalene based chemosensor **1** is shown in Scheme 1. Briefly, Schiff base reaction between

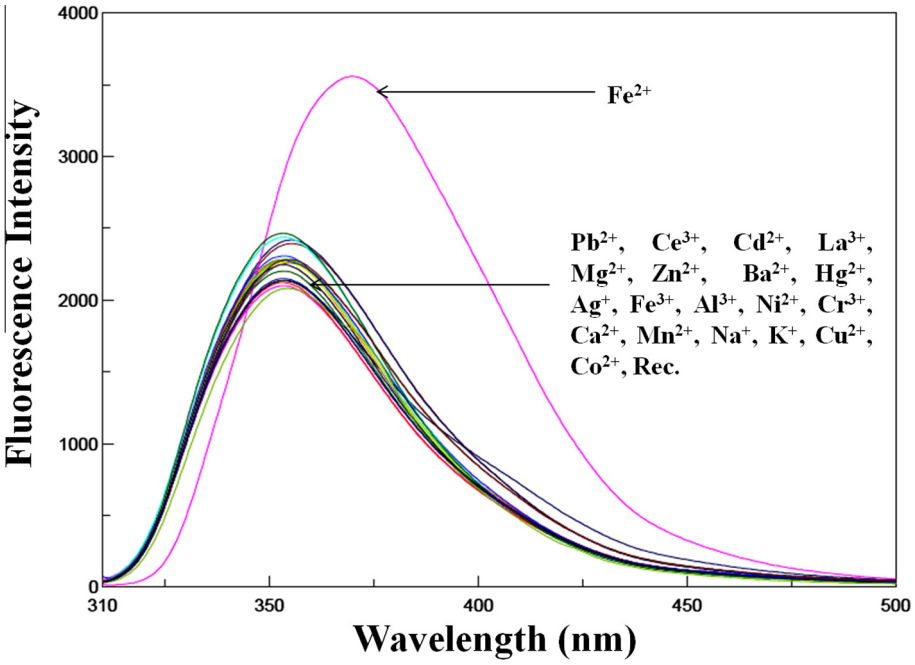

Fig. 1. Fluorescence spectral changes of **1** (4×10^{-6} M) $CH_3CN–H_2O$ solution (1:1 v/v, HEPES = 50 mM, pH = 7.4) in the presence of various metal ions (100 equiv. of each, λex. = 300 nm).

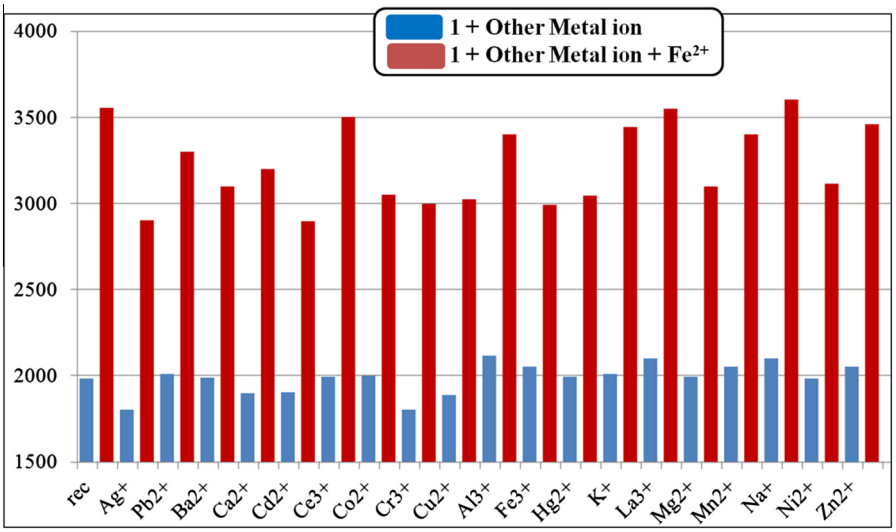

Fig. 2. Metal ions competition analysis of **1** (4×10^{-6} M) in CH_3CN–H_2O, (1:1 v/v, HEPES = 50 mM, pH = 7.4). The blue bars represent the fluorescence emission of **1** and 100 equiv. of other metal ions. The red bars represent the fluorescence changes that occur upon addition of 100 equiv. of other metal ions to the solution containing **1** and Fe^{2+} (100 equiv.). (For interpretation of the references to color in this figure legend, the reader is referred to the web version of this article.)

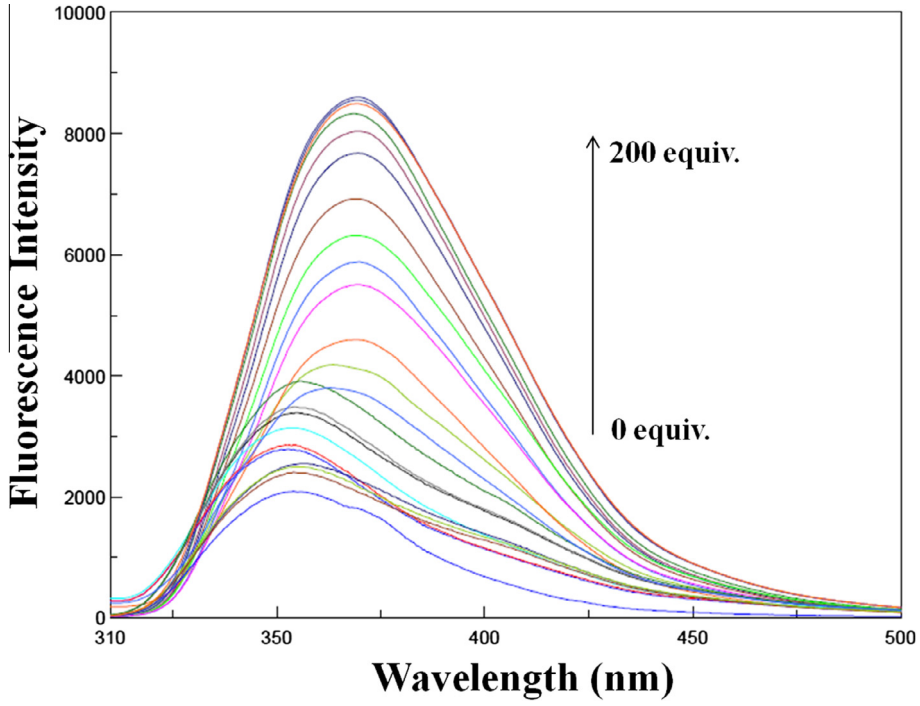

Fig. 3. Fluorescence titration spectrum of **1** (4×10^{-6} M) in CH_3CN–H_2O solution (1:1 v/v, HEPES = 50 mM, pH = 7.4) upon addition of different concentration of Fe^{2+} (0–200 equiv. of each, λex. = 300 nm).

1-naphthaldehyde and 2-aminopyridine in ethanol affords the crude **1** which is then purified by the recrystallization in methanol and characterized by the usual analytical and spectroscopic techniques (Figs. S1–S3).

3.2. Evaluation of selectivity

The UV–visible absorption spectrum of **1** in CH_3CN/H_2O (1:1 (v/v), HEPES = 50 mM, pH = 7.4) show two intense bands with absorption maximum at 225 and 300 nm (Fig. S4). Based on the absorption spectrum of **1**, the excitation was fixed at 300 nm for metal ion binding studies by fluorescence. Screening of the specific metal ion binding ability of sensor **1** was carried out in CH_3CN–H_2O (1:1 v/v, HEPES = 50 mM, pH = 7.4) solution. Sensor **1** showed a weak fluorescence. However, upon addition of 100 equiv. of Fe^{2+} to a solution of sensor **1**, two major things were observed. Firstly, the fluorescence enhancement and secondly, a notable red shift from 354 to 370 nm. The normalised spectrum clearly indicates the 16 nm bathochromic shift as shown in the Supporting information (Fig. S5). Nonetheless, under the same concentration (100 equiv.) of other metal ions such as Pb^{2+}, Cu^{2+}, Cd^{2+}, Hg^{2+}, La^{3+}, Zn^{2+}, Co^{2+}, Ni^{2+}, Ca^{2+}, Mn^{2+}, Cr^{3+}, Ba^{2+}, Ce^{3+}, Mg^{2+}, Al^{3+}, Fe^{3+}, Ag^{+}, Na^{+} and K^{+} addition to sensor **1**, produced some negligible changes in the fluorescence spectra (Fig. 1). As a result, **1** exhibits a selective

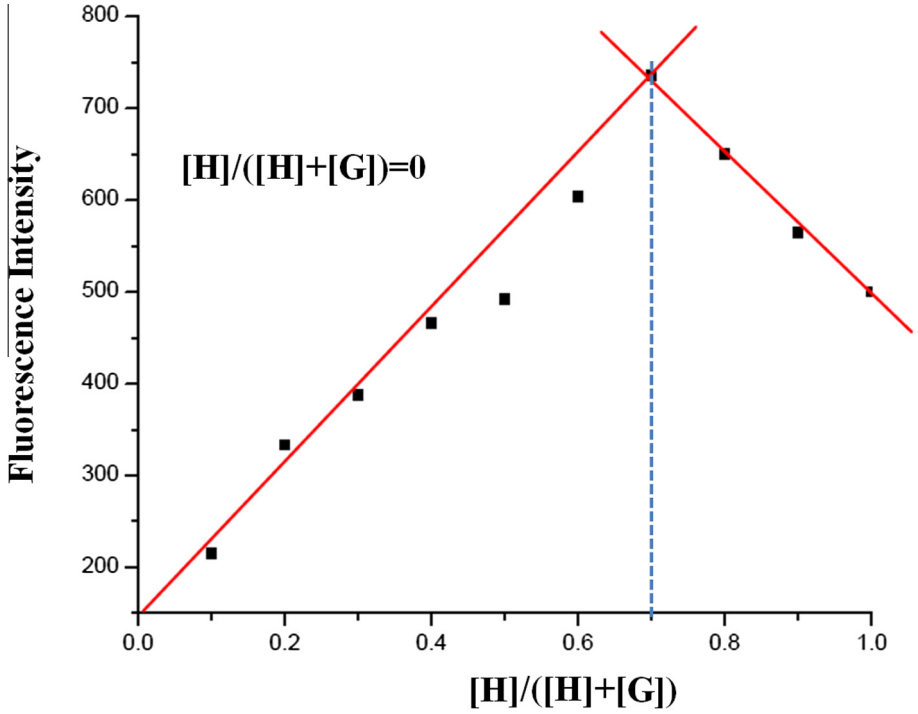

Fig. 4. Job plot of **1** and Fe^{2+} in $CH_3CN–H_2O$ solution (1:1 v/v, HEPES = 50 mM, pH = 7.4).

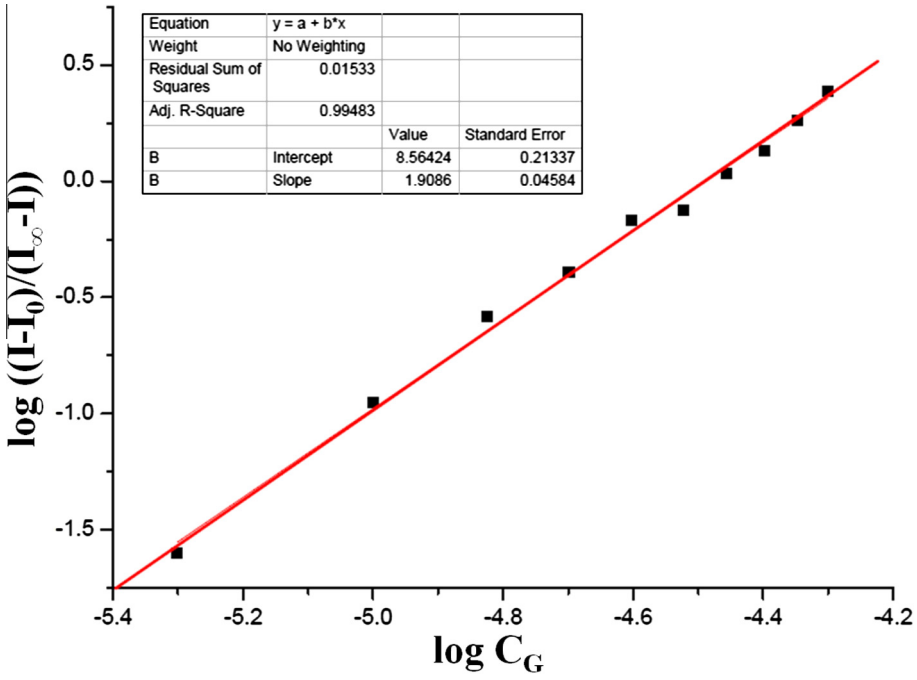

Fig. 5. Benesi–Hildebrand plot of **1**-Fe^{2+} complex (2:1) binding stoichiometry.

detection of Fe^{2+} when compared to other metal ions by a fluorescence turn-on response with notable red shift.

3.3. Effect of pH and time response

Sensitivity of **1** and **1** + **Fe^{2+}** at different pH values were studied to explore its photophysical properties in $CH_3CN–H_2O$ solution (1:1 v/v) (Fig. S6). The results showed that the sensor **1** exhibits a weak fluorescence over a wide range of pH except a small enhancement between 6 and 8 pH ranges. However, under identical conditions, on addition of Fe^{2+} to **1**, the fluorescence intensity gradually increases as the pH was varied from 0 to 6 and attains a maximum intensity at neutral condition. These results reveal that the Fe^{2+} recognition process is free from pH interference under the near neutral pH conditions. Thus, the physiological pH of 7.4 was selected as the working condition throughout the following spectroscopic experiments. Moreover, changes in fluorescence intensities of **1** to Fe^{2+} ($CH_3CN–H_2O$, 1;1 v/v, HEPES = 50 mM, pH = 7.4)

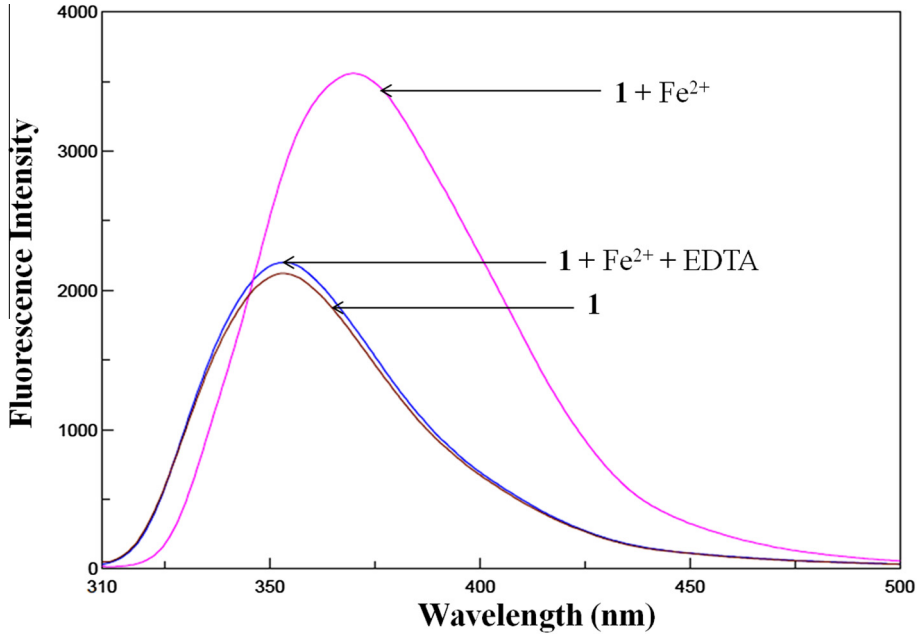

Fig. 6. Changes in fluorescent spectra of **1** (4×10^{-6} M) solution (CH_3CN–H_2O, 1:1 (v/v), HEPES = 50 mM, pH = 7.4) in the presence of Fe^{2+} & EDTA (100 equiv.).

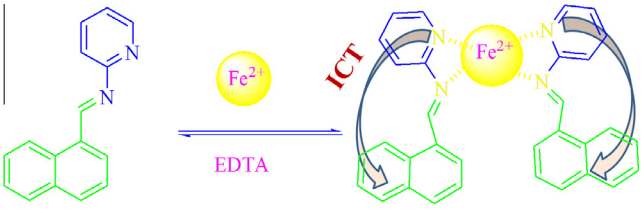

Scheme 2. Proposed binding mode of **1** with Fe^{2+}.

against time was performed (Fig. S7). However, sensor **1** with addition of Fe^{2+}, the fluorescence intensity increased and reached the maximum level within 2 min and kept steady for 50 min. From this study, it is clear that the sensor **1** can detect the Fe^{2+} in a short period of time of 2 min.

Furthermore to check the practical utility of sensor **1**, with the help of the competitive complexation analysis, the possible interferences by other co-existing metal ions were carried out. The fluorescence changes of **1** was measured by 100 equiv. of Fe^{2+} ions in the presence of same concentration of other interfering metal ions such as Na^+, K^+, Pb^{2+}, Cu^{2+}, Cd^{2+}, Hg^{2+}, La^{3+}, Zn^{2+}, Co^{2+}, Ni^{2+}, Ca^{2+}, Mn^{2+}, Cr^{3+}, Ba^{2+}, Ce^{3+}, Mg^{2+}, Al^{3+}, Fe^{3+} and Ag^+. The tested interfering metal ions showed no significant changes in the emission intensity for the detection of Fe^{2+} ion (Fig. 2). Hence, this result proved that the receptor **1** could be used for the selective detection of Fe^{2+}-ion in real sample sensing applications.

3.4. Stoichiometry and binding mode studies

In order to evaluate the binding ability and limit of detection of Fe^{2+} with **1**, the fluorescence titrations of **1** were performed by gradually increasing the concentration of Fe^{2+}. Fluorescence intensity was increased with increasing the concentration Fe^{2+} (0–200 equiv.) with a notable red shift (Fig. 3). Red shift was completed on the addition 100 equiv. of Fe^{2+} and the fluorescent profile changes was gradually enhanced and almost terminated upon the addition of 200 equiv. of Fe^{2+}, implying that **1** interacts with Fe^{2+} in 2:1 stoichiometry.

The mode of complexation between **1** and Fe^{2+} (Host–Guest) was confirmed by the Job's plot method [55,56]. Complex emission intensity was gradually increased with increasing the concentration of **1** as it reached a maximum mole fraction is 0.7. Afterwards, the intensity decreased with further addition of **1**, which eventually established a 2:1 (**1**:Fe^{2+}) binding stoichiometry (Fig. 4).

In addition, the binding stoichiometry between **1** and Fe^{2+} was also confirmed by the Benesi–Hildebrand nonlinear curve fitting method [57,58] (Fig. 5). The association constant was determined to be K_a 5.02×10^4 M^{-2} for the **1**–Fe^{2+} complex. The detection limit

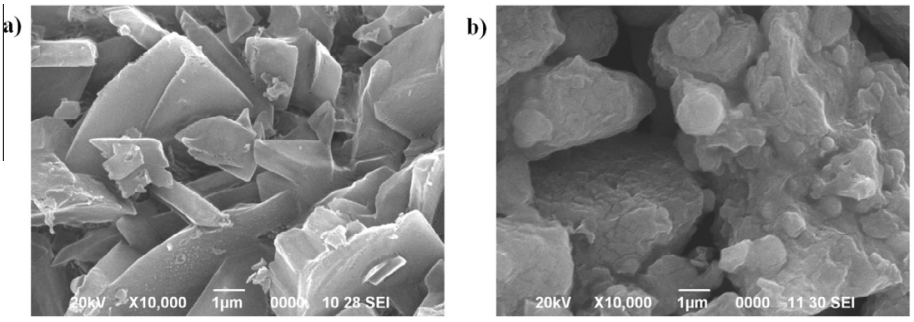

Fig. 7. SEM images of (a) **1** only and (b) **1** + $FeCl_2$.

Table 1
Determination of Fe^{2+} in real samples.

Sample	Amount of Fe^{2+} present in blank ppm (AAS)	Fe^{2+}-ion spiked (ppm)	Fe^{2+}-ion found (ppm) (Fluorescence) (Mean ± S.D.)	Recovery (%)
Tablet-1	100	0	100.82 ± 0.03	100.8
Tablet-2	50	0	50.24 ± 0.08	100.4
Tomato juice	02.7	0	02.52 ± 0.05	93.3
Dark chocolate	06.2	0	06.02 ± 0.03	97.0
Tap water-1	21	0	21.53 ± 0.02	102.5
Tap water-2	18	0	18.87 ± 0.04	104.8

Table 2
Comparison of reported iron sensors in different methods.

Refs.	Detected elements	LOD	Methods of detections
[21]	Fe^{2+}	12 nm	Fluorescence
[22]	Fe^{2+}	120 mmol/L	Fluorescence
[23]	Fe^{3+}	10^{-7} M	Graphite furnace AAS
[24]	Iron	0.50 mg L^{-1}	Multi-syringe flow injection system
[25]	Iron	7.7×10^{-9} M	Voltammetry
[26]	Fe^{3+}	0.1 ppm	Colorimetry naked-eye, Hydrogel sensor
[27]	Iron	0.02 μg L^{-1}	Flow injection spectrophotometric method
[44]	Fe^{2+}	3.6×10^{-6} M	Fluorescence
[47]	Fe^{3+}	–	Fluorescence
[48]	Fe^{3+}	5 μM	Fluorescence
[51]	Fe^{3+}	0.1 μM	Fluorescence
This work	Fe^{2+}	1.5×10^{-7} M	Fluorescence

of **1**, calculated using the formula $3\delta/S$ [59,60], is 1.5×10^{-7} M, where δ is the standard deviation of the blank signal, and S is the slope of the linear calibration plot.

3.5. Reversibility studies

The recognition and reversibility of a sensor **1** is an important requirement. Here, we examined the reversibility of the binding between **1** and Fe^{2+} in the presence of EDTA (100 equiv.) in CH_3CN–H_2O (1:1 (v/v), HEPES = 50 mM, pH = 7.4) solutions. The addition of EDTA (100 equiv.) to the solution of **1** containing Fe^{2+} led to the disappearance of the fluorescence signals of **1**-Fe^{2+} and attained the original intensity of free sensor **1**, indicating that the chelation process is reversible as shown in Fig. 6. The completion of the reversible process between Fe^{2+} with EDTA is 2 min.

3.6. Proposed binding mode of the complex

Based on the above mentioned results, a possible sensing mechanism for the detection of Fe^{2+} by the sensor is proposed and illustrated in Scheme 2. Sensor **1** with weak fluorescence intensity, exhibits a "turn-on" response with high fluorescence intensity on the addition of Fe^{2+} with a notable red shift. This may be due to the Intramolecular Charge Transfer (ICT) process between the naphthalene and pyridine moiety which are covalently linked through an imine bond (Schiff base). In addition to the ICT, the increase in the fluorescence intensity after the addition of Fe^{2+} to sensor **1** is due to the Chelation enhanced fluorescene which also inhibits the C–N torsional rotation by making the complex a rigid one which eventually arrests the C=N isomerisation. Fe^{2+} coordination with the nitrogen of C=N led to the slight rearrangement of C=N, which influences the conjugation between C=N and naphthalene. Job's plot and nonlinear curve fitting (Benesi–Hildebrand) methods reveals that the possible binding ratio is 2:1 between **1** and Fe^{2+} complex. From all of the above data, it could possibly be deduced that the coordination modes of **1**-Fe^{2+} complex is 2:1(Host:Guest) binding stoichiometry.

3.7. Microscopic studies

Finally, the morphological changes of **1** and **1** + Fe^{2+} were analyzed by SEM images, which are shown in Fig. 7. A crystal like random molecular size morphology was detected in sensor **1**. However, upon addition of Fe^{2+}, the size of the complex molecular size became smaller and agglomerated due to the formation of **1** + Fe^{2+} complex. This result further corroborates to the above discussions as the sensor **1** selectively detects Fe^{2+}-ions among all the other metal ions tested.

3.8. Application studies

As a practical applicability, we have examined the feasibility of **1** for the determination of the most abundant ion Fe^{2+} in different samples *via* fluorescence techniques. Six numbers of samples were analyzed by this method and these include commercially available tablets, tomato juice, dark chocolate and tap water (Table 1). As a result, the quantitative recoveries of non-spiked samples were satisfactory and confirmed with known standards. This indicates that **1** could potentially be used for the determination of Fe^{2+}-ion in real samples without any other co-existing metal ion interferences (Table 2).

4. Conclusion

In conclusion, a naphthalene derived fluorescent chemosensor **1** was developed for the detection of Fe^{2+} ions in CH_3CN–H_2O solution with lower detection limit of 1.5×10^{-7} M. The sensor **1** specifically recognizes Fe^{2+} over other heavy and transition metal ions including Fe^{3+}. The "turn-on" response followed by a notable red shift for recognition of Fe^{2+} by **1** is due to the ICT process and C=N isomerisation. In future, the sensor **1** could be used as a potential probe for the detection Fe^{2+} ions in biological and environmental monitoring works.

Acknowledgement

This work is supported by the Fast Track Programme for the young Scientists of the DST (No. SR/FT/CS-95/2010).

Appendix A. Supplementary material

Supplementary data associated with this article can be found, in the online version, at http://dx.doi.org/10.1016/j.ica.2015.09.030.

References

[1] J.S. Kim, D.T. Quang, Chem. Rev. 107 (2007) 3780.
[2] S.J. Lippard, J.M. Berg, Principles of Bioinorganic Chemistry, University Science Books, 1997.
[3] H.N. Kim, M.H. Lee, H.J. Kim, J.S. Kim, J. Yoon, Chem. Soc. Rev. 37 (2008) 1465.
[4] P. Aisen, M. Wessling-Resnick, E.A. Leibold, Curr. Opin. Chem. Biol. 3 (1999) 200.
[5] X. Chen, T. Pradhan, F. Wang, J.S. Kim, J. Yoon, Chem. Rev. 112 (2011) 1910.
[6] G.C. Kabat, T.E. Rohan, Cancer Causes Control 18 (2007) 1047.
[7] A. Ilari, M.C. Latella, P. Ceci, F. Ribacchi, M. Su, L. Giangiacomo, E. Stefanini, N.D. Chasteen, E. Chiancone, Biochemistry 44 (2005) 5579.
[8] M. Costas, M.P. Mehn, M.P. Jensen, L. Que, Chem. Rev. 104 (2004) 939.
[9] T.A. Rouault, W.-H. Tong, Nat. Rev. Mol. Cell Biol. 6 (2005) 345.
[10] E.C. Theil, D.J. Goss, Chem. Rev. 109 (2009) 4568.
[11] G. Papanikolaou, K. Pantopoulos, Toxicol. Appl. Pharmacol. 202 (2005) 199.
[12] K.J. Hintze, E.C. Theil, Proc. Natl. Acad. Sci. U.S.A. 102 (2005) 15048.
[13] T.B. Chaston, D.R. Richardson, Am. J. Hematol. 73 (2003) 200.
[14] M. Chen, H. Xiong, W. Wen, X. Zhang, H. Gu, S. Wang, Electrochim. Acta 114 (2013) 265.
[15] J.E.T. Andersen, Analyst 130 (2005) 385.
[16] P.J. Aggett, C. Agostoni, I. Axelsson, J.L. Bresson, O. Goulet, O. Hernell, B. Koletzko, H.L. Lafeber, K.F. Michaelsen, J. Micheli, J. Rigo, H. Szajewska, L.T. Weaver, Nutrition 34 (2002) 337.
[17] A.J. Weerasinghe, C. Schmiesing, S. Varaganti, G. Ramakrishna, E. Sinn, J. Phys. Chem. B 114 (2010) 9413.
[18] L.A. Ba, M. Doering, T. Burkholz, C. Jacob, Metallomics 1 (2009) 292.
[19] W. Breuer, M. Shvartsman, Z.I. Cabantchik, Int. J. Biochem. Cell Biol. 40 (2008) 350.
[20] G.J. Anderson, C.D. Vulpe, Cell. Mol. Life Sci. 66 (2009) 3241.
[21] P. Li, L. Fang, H. Zhou, W. Zhang, X. Wang, N. Li, H. Zhong, B. Tang, Chem. Eur. J. 17 (2011) 10520.
[22] P. Li, H. Xiao, B. Tang, Chin. J. Chem. 30 (2012) 1992.
[23] A. Ohashi, H. Ito, C. Kanai, H. Imura, K. Ohashi, Talanta 65 (2005) 525.
[24] D.M.C. Gomes, M.A. Segundo, J.L.F.C. Lima, A.O.S.S. Range, Talanta 66 (2005) 703.
[25] A. Bobrowski, K. Nowak, J. Zarebski, Anal. Bioanal. Chem. 382 (2005) 1691.
[26] H. Ozay, O. Ozay, Chem. Eng. J. 232 (2013) 364.
[27] S. Lunvongsa, M. Oshima, S. Motomizu, Talanta 68 (2006) 969.
[28] L.M. Moretto, J. Chevalet, G.A. Mazzocchin, P. Ugo, J. Electroanal. Chem. 498 (2001) 117.
[29] C. Huang, Z. Jiang, B. Hu, Talanta 73 (2007) 274.
[30] C. Karadas, D. Kara, A. Fisher, Anal. Chim. Acta 689 (2011) 184.
[31] M. Saleem, R. Abdullah, A. Ali, B.J. Park, E.H. Choi, I.S. Hong, K.H. Lee, Bioorg. Med. Chem. 22 (2014) 2045.
[32] Y. Shiraishi, S. Sumiya, Y. Kohno, T. Hirai, J. Org. Chem. 73 (2008) 8571.
[33] Y. Yan, Z. Che, X. Yu, X. Zhi, J. Wang, H. Xu, Bioorg. Med. Chem. 21 (2013) 508.
[34] Y. Xiang, A. Tong, Org. Lett. 8 (2006) 1549.
[35] D. En, Y. Guo, B.-T. Chen, B. Dong, M.-J. Peng, RSC Adv. 4 (2014) 248.
[36] A.-L. Bulteau, H.A. O'Neill, M.C. Kennedy, M. Ikeda-Saito, G. Isaya, L.I. Szweda, Science 305 (2004) 242.
[37] H. Shi, K.Z. Bencze, T.L. Stemmler, C.C. Philpott, Science 320 (2008) 1207.
[38] I.J. Schultz, C. Chen, B.H. Paw, I. Hamza, J. Biol. Chem. 285 (2010) 26753.
[39] D.R. Richardson, D.J.R. Lane, E.M. Becker, M.L.-H. Huang, M. Whitnall, Y.S. Rahmanto, A.D. Sheftel, P. Ponka, Proc. Natl. Acad. Sci. U.S.A. 107 (2010) 10775.
[40] R.C. Hider, X. Kong, Dalton Trans. 42 (2013) 3220.
[41] B. Halliwell, J.M.C. Gutteridge, FEBS Lett. 307 (1992) 108.
[42] I. Yamazaki, L.H. Piette, J. Biol. Chem. 265 (1990) 13589.
[43] S. Enami, Y. Sakamoto, A.J. Colussi, Proc. Natl. Acad. Sci. U.S.A. 111 (2014) 623.
[44] L. Praveen, M.L.P. Reddy, R.L. Varma, Tetrahedron Lett. 51 (2010) 6626.
[45] J.-L. Chen, S.-J. Zhuo, Y.-Q. Wu, F. Fang, L. Li, C.-Q. Zhu, Spectrochim. Acta Part A Mol. Biomol. Spectrosc. 63 (2006) 438.
[46] G.-G. Hou, C.-H. Wang, J.-F. Sun, M.-Z. Yang, D. Lin, H.-J. Li, Biochem. Biophys. Res. Commun. 439 (2013) 459.
[47] R. Wang, F. Yu, P. Liu, L. Chen, Chem. Commun. 48 (2012) 5310.
[48] Z. Yang, M. She, B. Yin, J. Cui, Y. Zhang, W. Sun, J. Li, Z. Shi, J. Org. Chem. 77 (2012) 1143.
[49] T.M. Geng, R.Y. Huang, D.Y. Wu, RSC Adv. 4 (2014) 46332.
[50] G. Sivaraman, V. Sathiyaraja, D. Chellappa, J. Lumin. 145 (2014) 480.
[51] M.H. Lee, T.V. Giap, S.H. Kim, Y.H. Lee, C. Kang, J.S. Kim, Chem. Commun. 46 (2010) 1407.
[52] H.M. Park, B.N. Oh, J.H. Kim, W. Qiong, I.H. Hwang, K.-D. Jung, C. Kim, J. Kim, Tetrahedron Lett. 52 (2011) 5581.
[53] F. Wang, R. Nandhakumar, J.H. Moon, K.M. Kim, J.Y. Lee, J. Yoon, Inorg. Chem. 50 (2011) 2240.
[54] J. Prabhu, K. Velmurugan, R. Nandhakumar, J. Lumin. 145 (2014) 733.
[55] L. Tang, N. Wang, Q. Zhang, J. Guo, R. Nandhakumar, Tetrahedron Lett. 54 (2013) 536.
[56] F. Wang, J.H. Moon, R. Nandhakumar, B. Kang, D. Kim, K.M. Kim, J.Y. Lee, J. Yoon, Chem. Commun. 49 (2013) 7228.
[57] K. Velmurugan, J. Prabhu, L. Tang, T. Chidambaram, M. Noel, S. Radhakrishnan, R. Nandhakumar, Anal. Methods 6 (2014) 2883.
[58] L. Tang, M. Cai, Z. Huang, K. Zhong, S. Hou, Y. Bian, R. Nandhakumar, Sens. Actuators, B 185 (2013) 188.
[59] K. Velmurugan, A. Raman, S. Easwaramoorthi, R. Nandhakumar, RSC Adv. 4 (2014) 35284.
[60] F. Wang, R. Nandhakumar, Y. Hu, D. Kim, K.M. Kim, J. Yoon, J. Org. Chem. 78 (2013) 11571.